Digital Holographic Printing Methods for 3D Visualization of Cultural Heritage Artifacts

Hoonjong Kang[1], Elena Stoykova[1,2], Nataliya Berberova[2], Jiyong Park[1], Youngmin Kim[1], Joo Sup Park[1], Sunghee Hong[1], Branimir Ivanov[2], Dimana Nazarova[2], Nikola Malinowski[2]

[1] Realistic Media Platform Research Center, Korea Electronics Institute of Technology, 8 Floor, #1588, Sangam-dong, Mapo-gu, Seoul, 121-835, Korea
[2] Institute of Optical Materials and Technologies, Bulgarian Academy of Sciences, Acad. Georgi Bonchev Str., Bl.109, 1113 Sofia, Bulgaria
natali.berberova@gmail.com

Abstract. Holography enables capture and reconstruction of the optical field scattered from three-dimensional (3D) objects. The hologram encodes both amplitude and phase of the field under coherent illumination, whereas photography records only the amplitude by incoherent light. 3D visualization feature of holography motivates expansion of research efforts dedicated to digital holographic imaging methods as a holographic display or a holographic printer. The paper presents two holographic 3D printing techniques which combine digital 3D representation of an object with analog holographic recording. Generation of digital contents is considered for a holographic stereogram printer and a recently proposed wavefront printer. These imaging methods could be applied to specific artifacts which are difficult to be recorded by conventional analog holography.

Keywords: igital holography, 3D imaging, holographic printing.

1 Introduction

Holography enables capture and reconstruction of the optical field scattered from three-dimensional (3D) objects [1]. This field is described by a complex amplitude $O(x,y,z)=a_O(x,y,z)\exp[j\varphi_O(x,y,z)]$ where (x,y,z) are Cartesian coordinates and "j" denotes imaginary unit. The quantity $I \equiv |a_O|^2$ gives the intensity of the scattered light whereas the phase φ_O carries information about the depth of the object. The hologram encodes both amplitude, $a_O(x,y,z)$, and phase, $\varphi_O(x,y,z)$, of the field under coherent illumination, whereas photography records only the amplitude, $a_O(x,y,z)$, by incoherent light. Thus holography allows for 3D imaging and metrology by phase decoding methods while the depth information is lost in conventional photography.

3D visualization feature of holography motivates research efforts dedicated to holographic imaging techniques. Among them, the most popular is recording of white-light viewable holograms into a light-sensitive media [2]. This so-called analog display holography is widely exploited. It contributes to the cultural tourism by making possible to arrange portable or permanent exhibitions of holograms which provide highly realistic 3D images of unique and valuable artifacts. Over the last two decades, with advances in optical sensors and computers, digital holography revealed its potential for developing 3D imaging techniques as a holographic display or a holographic printer to name a few. The holographic printing combines digital and analog holography by recording a hologram onto a holographic emulsion from digital contents [3]. This can be used for printing of analog holograms of virtual objects generated from computer-graphic models thus increasing the versatility of holographic recording. The aim of this paper is to describe 3D contents generation for holographic printing of cultural artifacts. Holographic printing can be applied to specific artifacts which are difficult to be recorded by conventional analog holography.

2 Holographic Recording Techniques

Interference of the object wave field, $O(x,y) = a_O(x,y)\exp[j\varphi_O(x,y)]$, which carries information about the object, and the mutually coherent reference field with a complex amplitude, $R(x,y) = a_R(x,y)\exp[j\varphi_R(x,y)]$, results in four terms superimposed in the hologram plane (x,y)

$$I_H(x,y) = |O(x,y) + H(x,y)|^2 = OO^* + RR^* + OR^* + RO^* \quad (1)$$

where the asterisk denotes a complex conjugate operator. The first and the second terms are the intensities I_O and I_R of the reference and object waves that form the zero-order term. The last two terms represent +1 and -1 diffraction orders which encode the relevant information about the phase:

$$I_H(x,y) = I_O + I_R + 2\sqrt{I_O I_R}\cos(\varphi_O - \varphi_R) \quad (2)$$

To fulfill the condition for mutual coherence, the object and reference light beams come from the same laser source. Thus the 2D real-valued hologram (1) or (2) contains information about the phase of the light wavefront coming from the 3D object as a 2D fringe pattern.

The most widely used for cultural heritage dissemination is recording of volume-type reflection holograms because they provide high-quality object reconstruction which could be observed in a wide viewing angle under illumination with a point source of white light [2,4]. Figure 1 shows two such holograms recorded in IOMT-BAS with a DPSS laser at 532 nm wavelength onto a silver-halide holographic plate. The holograms are exhibited in the Regional History Museum of Kardjali, Bulgaria. As the actual size of some of the recorded artifacts was very small to be observed by a bare eye, we positioned a magnifying glass in front of them during the recording.

However, such an approach has its shortcomings. The required magnification depends on the size of the object. In addition, using a magnifying glass may introduce distortions in the reconstructed image. A hologram of such objects can be done by applying a holographic printing technique which allows for digital increasing of the object size and further recording of analog white light viewable hologram of the increased object.

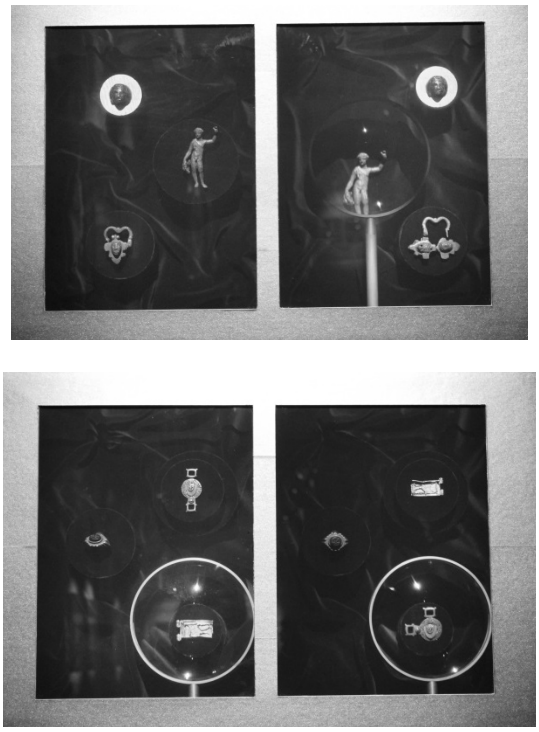

Fig. 1. Reflection holograms recorded on a silver-halide emulsion. Top: mask, statue of Dionysus, padlock; bottom: gold ring, gold application, silver buckle. (Regional History Museum of Kardjali, Bulgaria).

A common feature of holographic printers is division of the printed hologram into (2D) array of elemental volume-type reflection holograms or holographic elements (hogels) [5]. The digital content to be recorded in a hogel is displayed on a spatial light modulator (SLM). Recording of the whole hologram is done by successive exposure of all hogels using a motorized X-Y translation stage. Up to now, most of the printers work with a silver-halide or polymer light-sensitive emulsion. Below we discuss 3D digital contents generation for two types of printers – a holographic stereogram printer and a wavefront printer.

3 Digital Contents Generation for a Holographic Stereogram Printer

Strong visual impact of a holographic stereogram (HS) makes it a popular autostereoscopic display device which implement the idea of displaying a 3D scene by using stereo-images and the property given by Eqs.(1) and (2) of the holographic medium to record 3D wavefront through interference and to reconstruct it by diffraction [5]. The underlying technology behind the HS allows high-quality quasi-holographic 3D imaging of large objects. To make a HS, a sequence of 2D images of the scene is incoherently acquired from multiple views. The directional information carried by these perspective images is processed to form parallax-related images. The latter are displayed by the SLM and recorded onto a holographic photo-sensitive material by a laser as a volume-type hologram. The parallax-related images modulate the intensity of the object beam, $O(x, y)$. The whole hologram is divided into hogels which are sequentially exposed to the parallax-related images. Illumination of the fringe pattern recorded in the hologram for reconstruction of the 3D scene ensures spatial multiplexing of the perspective views. The viewer's left and right eyes observe different perspectives of the scene, as viewed from different directions, so the viewer perceives stereoscopic vision due to the binocular parallax.

Acquisition of the perspective images needs a tracking camera or modeling by a computer using different rendering methods. It is also possible to combine captured images with digitally rendered. The images are further processed to be recorded as hogels. At proper acquisition of the perspective images the HS can provide the viewer with an animated image. The large format printed holographic stereograms can be used to reconstruct in 3D the cultural and historical buildings and sites. The nowadays HSs, printed by the modern holographic printers, can boast with size up to 1 m × 1.5 m and field of view (FOV) about 100 degrees [6]. In this case the camera takes images along the horizontal axis only, and no acquisition is made along the vertical axis. The printed hologram exhibits only the horizontal parallax. In the case of a single artifact of small size, to print a full parallax hologram, the camera should take images along both horizontal and vertical axes. The recent advances in SLMs make possible fabrication of HSs with a very high spatial resolution. This entails capture or modeling of thousands of perspective images. The acquisition and post-processing of the perspective images can be entirely separated in space and time from the holographic recording. The hogel encodes information from a large number of pixels which correspond to the number of perspective images.

The simple and recentering camera methods were developed for acquisition of perspective images [7]. In the simple camera method the forward facing camera, preferably with a large FOV, captures perspective images, while being translated equidistantly along the horizontal or/and vertical axis. The simplicity of rendering of this method is counter-balanced by worsened resolution and unavoidable non-informative area in the acquired images. In addition, the camera with a large CCD and a large FOV lens is required. The latter may introduce severe distortions in the captured images. The recentering camera positions the acquired objects in the center of the images. This approach is much more efficient when it is used for capture of virtual objects. The virtual object can be built from a computer-graphic model created from a cloud of points extracted from a real object captured by holographic or profilometric means [8].

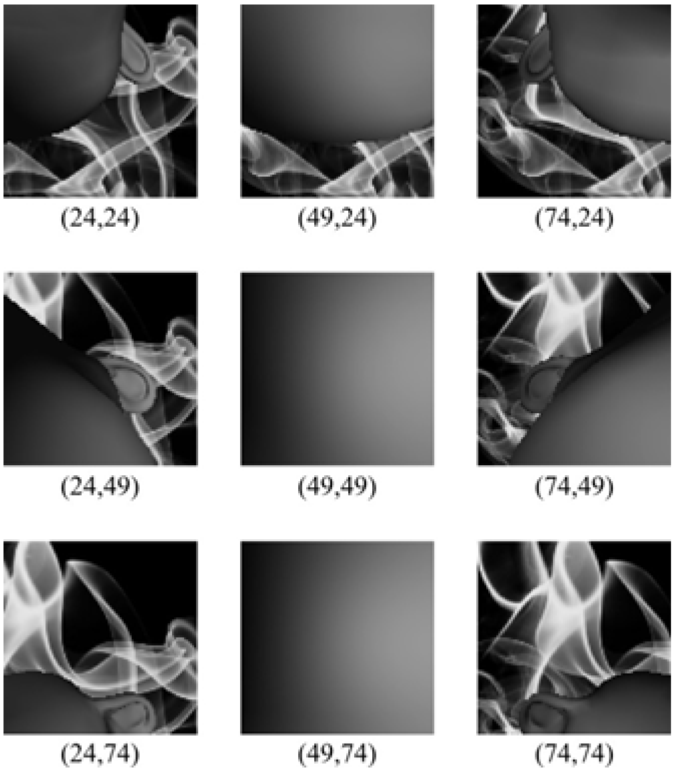

Fig. 2. Hogel images corresponding to different coordinates of hogels in the holographic plane; the numbers give the indices i and j in Eq.(3).

To view distortion-free reconstruction, perspective images should be rearranged to form the separate parallax or “hogel" images corresponding to different hogels in the hologram plane. Both perspective and hogel images are 2D arrays with, in general, different dimensions. The perspective images $P_{kl}, k=1..n, l=1..m$ compose a stack Φ of $n \times m$ images, where n and m are the number of images captured in horizontal and vertical directions, and k and l are indices of the camera positions at image capture. Each perspective image consists of $N \times M$ pixels. The size of the hogel images is $n \times m$ whereas their number is given by $N \times M$. The pixels in the hogel images are arranged in the order of capture of perspective images along horizontal and vertical axes. The hogel image h_{ij} is composed from (i,j)-th pixels in all perspective images in Φ as follows:

$$h_{ij}(k,l) = P_{kl}(i,j), k = 1..n, l = 1..m; i = 1..N, j = 1..M \quad (3)$$

Figure 2 depicts examples of hogel images to be recorded in different hogels. These hogel images were composed from 100 by 100 perspective images acquired from a small object positioned in front of a color background. The recentering camera model was used to simulate capture of perspective images. Each hogel image consists of three images obtained for the primary colors. The total number of hogel images was also 100 by 100. The HS reconstructed by numerical simulation at different view-points is shown in Fig.3. We see that reconstruction exhibits horizontal and vertical parallax which proves that the HS printing approach is suitable for full parallax color visualization of artifacts provided they are captured from multiple camera positions or their computer-graphics models are built from capture data acquired by other 3D capture methods.

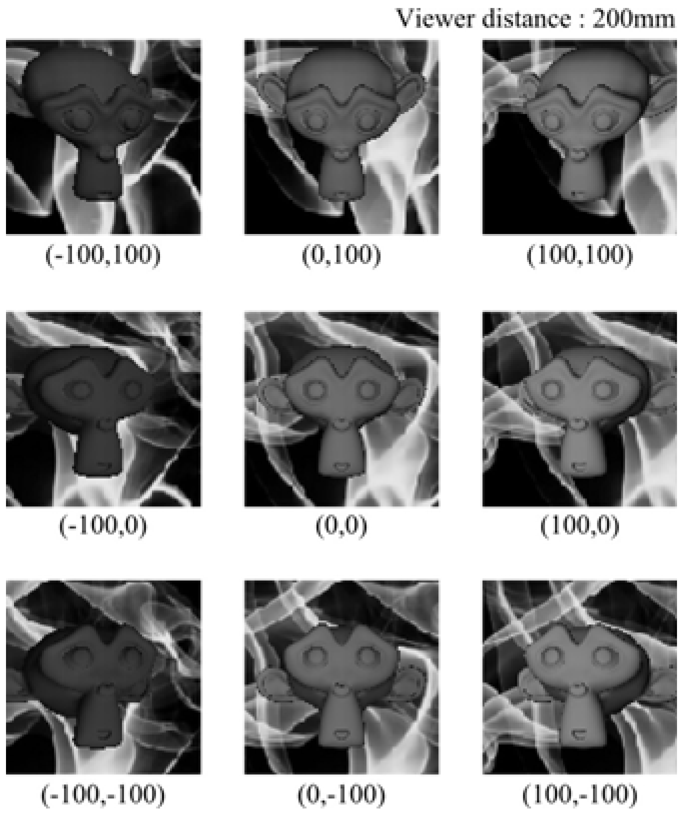

Fig. 3. Numerical reconstructions of a holographic stereogram from different viewpoints; the numbers give the coordinates of the viewpoint in millimeters; (0,0) is the central view-point.

4 3D Contents Generation for a Wavefront Printer

Similarly to the conventional analog hologram, the wave-front printer records the light field scattered from a 3D object [9-11]. This light field is encoded in a computer generated fringe pattern given by Eqs.(1) and (2). The small part of this fringe pattern corresponding to a hogel is fed to a SLM. The light field diffracted from the SLM is appropriately filtered to extract only the wavefront of light coming from the object. This wavefront is recorded as a volume reflection elemental hologram. In the systems using an amplitude-type SLM both zero-order and -1st diffraction order are cut off [9-11]. By updating the information displayed on the SLM and using a motorized X-Y stage a large hologram is composed.

The fringe pattern to be displayed on the SLM should mimic the optical recording of the hologram. For the purpose the object is considered as a set of self-emitting points. Each of them is a source of a spherical wavefront (Fig.4). The exact fringe pattern is given by digital implementation of the Rayleigh-Sommerfeld (R-S) diffraction integral which describes the complex amplitude of the object light field at the point (ξ, η) in the plane of the hologram as a sum of the spherical waves coming from all points of the object:

$$O(\xi, \eta) = \sum_{p=1}^{N} \frac{a_p}{r_p} \exp\left[j\left(kr_p + \varphi_p\right)\right] \tag{4}$$

$$r_p = \sqrt{\left(x_p - \xi\right)^2 + \left(y_p - \eta\right)^2 + z_p^2} \tag{5}$$

where the expression $\frac{a_p}{r_p} \exp\left[j\left(kr_p + \varphi_p\right)\right]$ is the description of the spherical wave coming from the object's point with the Cartesian coordinates (x_p, y_p, z_p), a_p and φ_p are the amplitude and the phase of this wave, and r_p is the distance between this point and the point on the hologram; $k = 2\pi/\lambda$ is a wave number, λ is the wavelength. Computer generation of the hologram given by Eq.(1) allows to keep the only relevant term which is $H = 2\,\mathrm{Re}\{OR^*\}$, that allows to calculate the fringe pattern of the so called bipolar intensity

$$H_{bi}(\xi, \eta) = \sum_{p=1}^{N} \frac{a_p}{r_p} \cos\left(kr_p + \varphi_p + \varphi_R\right) \tag{6}$$

by using only the real numbers where we assume that the amplitude of the reference wave a_R is equal to unity. However, one of the substantial drawbacks of the R-S method is its quite high computational complexity. To accelerate computation of the holographic fringe pattern we developed the fast phase-added stereogram (FPAS) method [12]. The hologram plane is divided into $M \times N$ square segments. The numerical model of the FPAS in each segment is expressed as

$$H_{mn}(\xi,\eta) = F^{-1}\{I_{mn}(u,v)\} \quad (7)$$

$$\begin{aligned} I_{mn}(u,v) = \sum_{p=1}^{P} \frac{a_p}{r_{pmn}} \exp\left[j\left(kr_{pmn} + \phi_p\right)\right] \times \\ \exp\left\{i2\pi\left[u_{pmn}\left(x-\xi_p\right) + v_{pmn}\left(\eta - y_p\right)\right]\right\}\delta\left(u-u_{pmn}, v-v_{pmn}\right) \end{aligned} \quad (8)$$

where $H_{mn}(\xi,\eta)$ is the holographic fringe pattern in the *mn*-th segment, and $I_{mn}(u,v)$ is its spatial frequency distribution in the spatial frequency domain, F^{-1} denotes 2D inverse fast Fourier transform. The distance r_{pmn} is determined with respect to the segment central point. The spatial frequencies u_{pmn} and v_{pmn} are also determined for the central point by $u_{pmn} = \lambda^{-1}\left(\sin\theta_{\xi pmn} - \sin\theta_{r\xi}\right)$, $v_{pmn} = \lambda^{-1}\left(\sin\theta_{\eta pmn} - \sin\theta_{r\eta}\right)$, where, $\theta_{\xi pmn}$ and $\theta_{\eta pmn}$ are the incident angles from a given object point, and $\theta_{\xi r}$ and $\theta_{\eta r}$ are the illuminating angles of the plane reference wave with respect to the ξ and η axes.

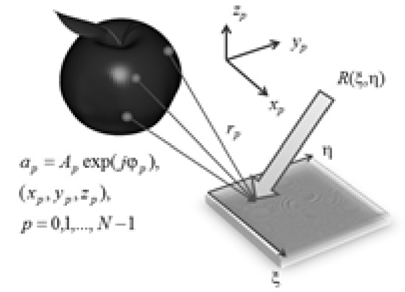

Fig. 4. Schematic representation of the Rayleigh-Sommerfeld approach for generation of digital contents for the wavefront printer.

Figure 5 presents black & white photos of several white light viewable full color reflection holograms computed and printed with a wavefront printer. The holograms were composed from 60 by 100 hogels. The amplitude-type SLM was used with resolution 1920 by 1080 pixels and pixel interval 7 micrometers. The fringe patterns were computed from point clouds derived from computer-graphic models at three wavelengths by using both R-S diffraction integral and FPAS method. The size of the printed holograms is 4 cm by 4 cm. The holograms were printed with the wavefront printer system developed in KETI (South Korea) by using red, green and blue lasers. All holograms in Fig.5 exhibit good reconstruction of pure colors. The hologram in Fig.5 (a) shows a green figure wandering in a red night under yellow stars. The image reconstructed from the second hologram in Fig. 5(b) reproduces well the white color of the plane model. The reconstructions in Fig.5(c) show horizontal and vertical parallax. The obtained results prove that the color wavefront printer is a suitable choice for producing holograms of specific objects.

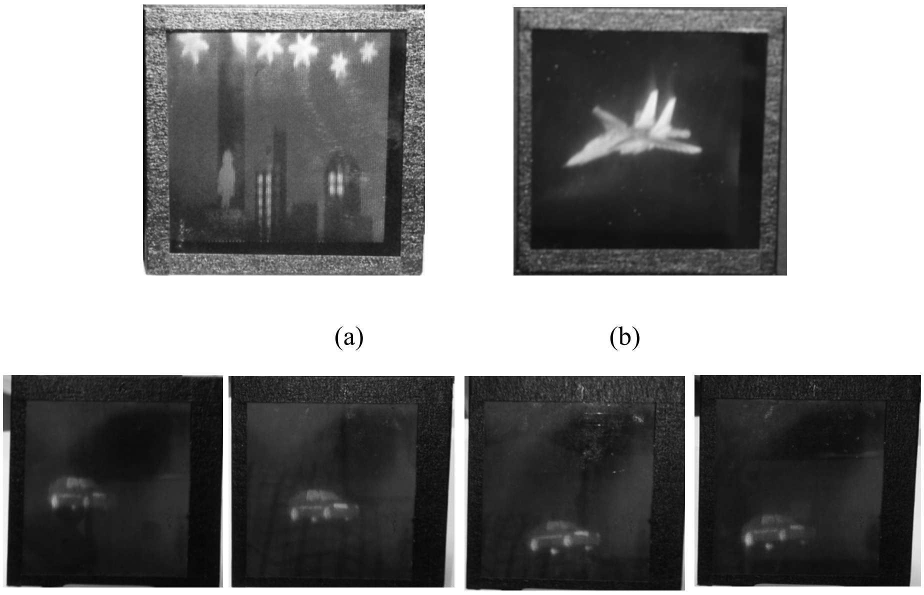

(a) (b)

(c)

Fig. 5. Black and white photos of white light viewable full color reflection holograms: (a) “Night of passion” by the holographic artist Ray Park (Joo Sup Park); (b) plane model; (c) different views of a toy car. All hologram are printed by a RGB wavefront printer, KETI (South Korea).

Acknowledgments

This work was supported by the IT R&D program of MSIP-Korea [Fundamental technology development for digital holographic contents], and the project "Perperikon - home of Gods and People", Bulgaria.

References

1. Stoykova, E., Kang, H., Park, J., Twin-image problem in digital holography-a survey (Invited Paper), Chin. Opt. Lett. 12, 060013- (2014)
2. Sainov, V., Stoykova, E., Display Holography – Status and Future, Chapter in a book Optical Imaging and Metrology: Advanced Technologies, First Edition. Edited by Wolfgang

Osten and Nadya Reingand. © 2012 Wiley-VCH Verlag GmbH & Co. KGaA., 93-117 (2012)

3. Yamaguchi, M, Ohyama, N, Honda, T, Holographic three-dimensional printer: new method, Appl. Opt. 31: 217-222 (1992)
4. Bjelkhagen H, Mirlis E. Color holography to produce highly realistic three-dimensional im-ages, Applied Optics, 47(4): A123-A133 (2008)
5. Kang, H., Stoykova, E., Park, J., Hong, S.H., Kim, Y., Holographic printing of white-light viewable holograms and stereograms, chapter 8, in Holography - Basic Principles and Con-temporary Applications, Ed. Emilia Mihaylova, ISBN 978-953-51-1117-7 (2013)
6. Brotherton-Ratcliffe D, Zacharovas S, Bakanas R, Pileckas J, Nikolskij A, Kuchin J., Digital holographic printing using pulsed RGB lasers, Optical Engineering; 50(9): 091307-091307-9 (2011)
7. Park, J., Stoykova, E., Kang, H., Hong, S., Lee, S., Jung, K., Numerical reconstruction of full parallax holographic stereograms, 3D Research 03, 03: 6 (2012)
8. Stoykova, E, Harizanova, J., Sainov,V., Pattern projection profilometry for 3D coordinates measurement of dynamic scenes, Chapter in the book “Three-dimensional television”, Springer, H.-M. Ozaktas, L.Onural, Eds., 85-164 (2008)
9. Yamaguchi, T., Miyamoto, O., Yoshikawa, H., Volume hologram printer to record the wavefront of three-dimensional objects, Opt.Eng. 51 (7), 075802 (2012)
10. Kang, H., Stoykova, E., Wave-field recording onto a holographic emulsion, Proc. Second Japan-Korea Workshop on Digital Holography and Information Photonics (2012)
11. Kang, H., Stoykova, E., Yoshikawa, H., Hong, S., Kim, Y., Comparison of system properties for wavefront holographic printers, Fringe 2013, W. Osten (ed.), Springer-Verlag Berlin Heidelberg (2014)
12. Kang, H., Stoykova, E., Partitioning based fast digital hologram generation method, Proc. Third Korea-Japan workshop on digital holography and information photonics (2013)